Simulation of high variable random processes through the spectral-representation-based approach

Pierfrancesco Cacciola
School of Environment and Technology, University of Brighton, Brighton, BN24GJ,
p.cacciola@brighton.ac.uk

Abstract: In this paper the traditional spectral-representation-method for simulating stochastic processes is revisited. A modification aimed to control the variability of the simulated samples of the random process is proposed. Specifically, in order to avoid that the simulated samples possess similar Fourier spectrum, it is proposed to randomize the power spectral density function through a pass band filter with random parameters. The filters is selected in such a way the ensemble averaged power spectral density determined by the samples will match the original power spectrum, but each individual sample will possess different frequency distributions. Comparison between the traditional simulation technique and the new one proposed in this paper will be also discussed. Results show that despite the ensemble averaged power spectral density is the same, related quantities, such as the distribution of peaks, will be significantly different highlighting the needing to consider the variability of frequency distributions when stochastic models are calibrated from experimental data.

Keywords: Monte Carlo simulation, variability, spectral-based representation

1. Introduction

Several problems in science and engineering involve uncertain quantities generally modeled as stochastic processes or stochastic fields. The evaluation of the response of structures to seismic or wind actions, the reliability of composite materials, the action potential generation in neurons, the drifting of particles suspended in fluids, the distribution of nanoparticles, the mutation of populations subjected to genetic drift are just few examples of the plethora of problems involving stochastic modeling. The solution of the stochastic problem is generally pursued through *ad hoc* strategies including simulation techniques, stochastic calculus and perturbation methods. The Monte Carlo simulation seems to be, up to now, the only universal method able to cope with different problems using a systematic approach: i) simulation of samples of the stochastic process (field), ii) solution of the deterministic problem for each individual sample, iii) statistical evaluation of the results. The simulation of the samples represents the first step and requires the definition of a proper stochastic model representing reliably the uncertainty embedded in the problem. Gaussian models are certainly the most used models used to represent and simulate stochastic processes especially for engineering applications. Accordingly, the Gaussian random process is fully defined by the mean and by power spectral density function (or alternatively by the mean and the autocorrelation function). Therefore, after defining a suitable model of the power spectral density the samples can be simulated through various techniques such as the spectral representation method (SRM), Karhunen-Loeve (KL) decomposition, ARMA models. In the framework of simulation of Gaussian processes (fields), the spectral representation method based on the superposition of harmonics with random

5th International Conference on Reliable Engineering Computing (REC 2012)
Edited by M. Vořechovský, V. Sadílek, S. Seitl, V. Veselý, R. L. Muhanna and R. L. Mullen

ISBN 978-80-214-4507-9. Published by Ing. Vladislav Pokorný − LITERA

phases (see e.g. Shinozuka and Deodatis, 1988) is certainly one of the most diffused approaches. This method has been applied in the last three decades to solve efficiently several problems in the fields of civil, mechanical and aeronautical engineering.

The increasing number of data collected from laboratory experiments or recorded through measuring stations and the sustained progress in experimental measurement techniques is compelling the research in stochastic modeling to validate (and eventually improve) models and the methodologies traditionally adopted by the comparison of observed and simulated random data. In the field of earthquake engineering, as an example, the increasing number of strong-motion networks installed worldwide revealed that the current methodologies for simulating artificial earthquakes possess the drawback that the simulated time-histories do not manifest large variability of the seismological parameters observed for natural accelerograms. As a consequence, the dispersion of the consequent structural response analysis can be underestimated. This issue has been recently addressed by calibrating some of parameters embedded in traditional stochastic models by using experimental data. Specifically, Pousse et al. (2006) proposed a methodology for simulating accelerograms through a stochastic approach by using the K-Net Japanese database. The basic idea of this approach is to define an evolutionary power spectral density function possessing random variables determined through empirical attenuation equations. Recently, Rezaeian and Der Kiureghian (2010) proposed a method for simulating synthetic ground motion time histories through a parameterized stochastic model based on a modulated filtered white-noise process. The parameters of the model are random variables calibrated on a set of recorded earthquakes. Cacciola and Zentner (2012) introduced the natural variability of ground motion accelerograms in the model through a pertinent evolutionary power spectrum with random coefficients. The distribution of the random coefficients has been determined by the further matching with a given mean ± standard deviation response spectra evaluated using an European earthquake database.

The above recent contributions addressed the issue of the discrepancy between the experimental and simulated samples including random parameter in the model. This approach leads to more realistic simulation that in general manifest greater dispersion in peak values and in general in the energy distribution. In this paper, based on the same motivations, the traditional spectral-representation-method for simulating stochastic processes is revisited. A modification aimed to control the variability of the simulated samples of the random process is proposed. Specifically, in order to avoid that the simulated samples possess the same Fourier spectrum, it is proposed to filter the power spectral density through a pass band filter with random parameters. The filters is selected in such a way the ensemble averaged power spectral density will match the original power spectrum, but each individual samples will possess different frequency distributions. Comparison between the traditional simulation technique and the new one proposed in this paper will be also discussed.

2. Simulation of random processes via the spectral representation method

In this section the spectral-representation-method (see e.g. Shinozuka and Deodatis, 1988, Deodatis 1996) is briefly described. The formulation will be based on stationary and non-stationary random process, but can be easily extended to homogeneous or non-homogeneous random field. Consider the one-dimensional and uni-variate Gaussian non-stationary stochastic process, $f(t)$, having zero mean:

$$E\left[f(t)\right]=0, \tag{1}$$

and the correlation function $R(t,t+\tau)$ given by the following equation

$$R(t,t+\tau)=E\left[f(t)f(t+\tau)\right]. \tag{2}$$

The process $f(t)$ can be defined alternatively by evolutionary power spectral density function defined (Priestley, 1965):

$$S(\omega,t)=\left|A(\omega,t)\right|^2 S(\omega)=\frac{1}{T}E\left[\left|\int_t^{t+T} f(\vartheta)e^{-i\omega\vartheta}\mathrm{d}\vartheta\right|^2\right] \tag{3}$$

being $(t,t+T)$ with $T<<t$ a *small* interval; also $A(\omega,t)$ and $S(\omega)$ are the (non-separable) modulating function and the (stationary) power spectral density function of the stochastic process, $f(t)$. It is noted that the ensemble average in equation (3) is not commonly used to define the evolutionary spectrum due the difficulties in its numerical evaluation related to the Uncertainty Principle and alternative representations of joint time-frequency representation are also proposed (see e.g. Spanos and Failla, 2004). Therefore, the evolutionary power spectral density is usually defined indirectly from the knowledge of the autocorrelation function, that is

$$S(\omega,t)=\frac{1}{2\pi}\int_{-\infty}^{\infty} R(t,t+\tau)e^{-i\omega\tau}\mathrm{d}\tau. \tag{4}$$

The correlation function therefore is related to the power spectral density function through the following transformation:

$$R(t,t+\tau)=\int_{-\infty}^{\infty} A(\omega,t)A(\omega,t+\tau)S(\omega)e^{i\omega\tau}\mathrm{d}\omega. \tag{5}$$

Due to the non-stationarity of the vector process, the autocorrelation function is function of both time t and time lag τ , while the power spectral density function is a function of both frequency ω and time t . It has to be emphasized that under the hypothesis of fully non-stationary processes (non-stationary processes with amplitude and frequency modulation), the power spectral density function is a non-separable function of frequency ω and time t . For the special case of uniformly modulated non-stationary stochastic process (or generally known also as quasi-stationary process), the modulating function $A(\omega,t)$ is independent of the frequency ω , that is:

$$A(\omega,t)=A(t). \tag{6}$$

In this special case, equation (5) reduces to

$$R(t,t+\tau)=A(t)A(t+\tau)\int_{-\infty}^{\infty} S(\omega)e^{i\omega\tau}\mathrm{d}\omega. \tag{7}$$

Finally in the case in which $A(t)=1$, i.e. stationary case, the following equations hold

$$R(\tau) = \int_{-\infty}^{\infty} S(\omega) e^{i\omega\tau} \mathrm{d}\omega; \tag{8}$$

$$S(\omega) = \frac{1}{2\pi} \int_{-\infty}^{\infty} R(\tau) e^{-i\omega\tau} \mathrm{d}\tau. \tag{9}$$

Equations (8) and (9) are generally known as the Wiener-Khintchin relationships. For the stationary case the power spectral density function can be also determined directly from experimental data

$$S(\omega) = \lim_{T\to\infty} \frac{1}{2\pi T} E\left[\left| \int_{-T/2}^{T/2} f(\vartheta) e^{-i\omega\vartheta} \mathrm{d}\vartheta \right|^2 \right]. \tag{10}$$

Once defined the power spectral density function either through experimental or physical/theoretical approaches the simulation of the sample of the non-stationary random process through the spectral representation method is performed using the following equation

$$f(t) = \sqrt{2} \sum_{j=1}^{N} \sqrt{2S(\omega_j, t)\Delta\omega} \cos\left(\omega_j t + \phi_j\right), \tag{11}$$

where

$$\omega_j = j\Delta\omega \qquad j = 1,2,...,N \tag{12}$$

with upper bound (circular) frequency $\omega_N = N\Delta\omega$ generally known also as the cut-off frequency beyond which the power spectral density function $S(\omega,t)$ is considered negligible. Also ϕ_j $(j = 1,2,...,N)$ are independent random variable distributed over the range $(0, 2\pi)$. The simulated process is asymptotically Gaussian as N tend to infinity due to the Central Limit Theorem. Also it can be shown (Shinozuka and Deodatis 1988, Deodatis 1996) that the ensemble averaged $E[f(t)]$ and $E[f(t)f(t+\tau)]$ tend to the corresponding target. Finally, samples of stationary processes can be simulated through equation (11) by substituting $S(\omega,t)$ with $S(\omega)$.

3. Enhancing the variability of the spectral representation method

It has emphasized that the simulation of random samples through the spectral representation method defined in equation (11) is based on the definition of the power spectral density function $S(\omega,t)$. Consider the power spectrum determined through the ensemble averages of experimental data (see e.g. Shillinger and Papadopoulos, 2011). Depending from the degree of randomness, the experimental data might exhibit strongly different distributions of the Fourier spectrum. In such a case, to better represent the underlying uncertainty , the simulated samples are expected not only converge to the target mean value and correlation function as equation (11) guarantees, but also it is expected that they manifest the variability of the spectrum around is expected value. In other words it is expected that the simulated data also capture the variability of the Fourier distribution of the experimental data. To enhance the variability of the simulated

random samples in this paper it is proposed to introduce a random filter acting in series with the expected value of the power spectrum, that is

$$S(\omega,t,\boldsymbol{\alpha}) = H(\omega,\boldsymbol{\alpha})S(\omega,t) \quad , \tag{13}$$

where $\boldsymbol{\alpha}$ is the vector collecting the random parameter of the filter. $H(\omega,\boldsymbol{\alpha})$ is real positive function that satisfies the following equation

$$\int_A S(\omega,t,\boldsymbol{\alpha})p_A(\boldsymbol{\alpha})\mathrm{d}\boldsymbol{\alpha} = \int_A H(\omega,\boldsymbol{\alpha})S(\omega,t)p_A(\boldsymbol{\alpha})\mathrm{d}\boldsymbol{\alpha} = S(\omega,t) \quad . \tag{14}$$

Or alternatively

$$\int_A H(\omega,\boldsymbol{\alpha})p_A(\boldsymbol{\alpha})\mathrm{d}\boldsymbol{\alpha} = 1 \quad \forall\,\omega\in\Omega \tag{15}$$

In equations (14) and (15) $p_A(\boldsymbol{\alpha})$ is the joint probability density function of random parameter of the filter. It is noted the proposed definition of the resultant random power spectrum is similar to the physical stochastic model recently defined by Li et al. (2012), but with different meaning. Embedding the proposed random spectrum in the traditional spectral representation method (SRM) the following simulation formula is herein derived

$$f_H(t) = \sqrt{2}\sum_{j=1}^{N}\sqrt{2H(\omega_j,\boldsymbol{\alpha})S(\omega_j,t)\Delta\omega}\cos\left(\omega_j t + \phi_j\right) \tag{16}$$

The samples generated by equation (16) are Gaussian as N tends to infinity due to the Central Limit Theorem and converge to the target mean $E\left[f_H(t)\right] = 0,$ and correlation function $R(t,t+\tau) = E\left[f_H(t)f_H(t+\tau)\right]$ as the traditional SRM.

Proof : the proof of convergence is based on the corresponding one proposed by Shinozuka and Deodatis (1988) and Deodatis (1996) to prove the convergence of equation (11). Due to the statistical independence of the random phase ϕ_j ($j = 1,2,...,N$) and assuming $\boldsymbol{\alpha}$ independent from ϕ_j , the expected value $E\left[f_H(t)\right]$ using equation (16) becomes

$$E\left[f_H(t)\right] = \int_A \int_0^{2\pi} \overset{N-\text{fold}}{\cdots} \int_0^{2\pi} \sqrt{2}\sum_{j=1}^{N}\sqrt{2H(\omega_j,\boldsymbol{\alpha})S(\omega_j,t)\Delta\omega}\cos\left(\omega_j t + \phi_j\right)p_A(\boldsymbol{\alpha})\left(\prod_{i=1}^{N} p_{\Phi_i}(\phi_i)\mathrm{d}\phi_i\right)\mathrm{d}\boldsymbol{\alpha}, \tag{17}$$

Where $p_{\Phi_i}(\phi_i)$ $(=1/2\pi,\ 0\le\phi_i\le 2\pi\ ;\ =0,\ \textit{otherwise})$ is the probability density function of ϕ_i . Rearranging terms in equation (17)

$$E\left[f_H(t)\right]=\sqrt{2}\sum_{j=1}^{N}\int_{A}\sqrt{H(\omega_j,\boldsymbol{\alpha})}p_A(\boldsymbol{\alpha})\mathrm{d}\boldsymbol{\alpha}\left[\int_0^{2\pi}\overset{N-\text{fold}}{\ldots}\int_0^{2\pi}\sqrt{2S(\omega_j,t)\Delta\omega}\cos\left(\omega_j t+\phi_j\right)\left(\prod_{i=1}^{N}p_{\Phi_i}(\phi_i)\mathrm{d}\phi_i\right)\right]=$$
$$=\sqrt{2}\sum_{j=1}^{N}\int_{A}\sqrt{H(\omega_j,\boldsymbol{\alpha})}p_A(\boldsymbol{\alpha})\mathrm{d}\boldsymbol{\alpha}\sqrt{2S(\omega_j,t)\Delta\omega}\left[\int_0^{2\pi}\frac{1}{2\pi}\cos\left(\omega_j t+\phi_j\right)\mathrm{d}\phi_i\right]=0 \tag{18}$$

The autocorrelation function of the simulated process

$$R(t,t+\tau)=E\left[f_H(t)f_H(t+\tau)\right]=$$
$$=\int_A\int_0^{2\pi}\overset{N-\text{fold}}{\ldots}\int_0^{2\pi}\sqrt{2}\sum_{i=1}^{N}\sum_{j=1}^{N}\sqrt{2H(\omega_i,\boldsymbol{\alpha})S(\omega_i,t)\Delta\omega}\sqrt{2H(\omega_j,\boldsymbol{\alpha})S(\omega_j,t)\Delta\omega} \tag{19}$$
$$\times\cos\left(\omega_i t+\phi_i\right)\cos\left(\omega_j(t+\tau)+\phi_j\right)p_A(\boldsymbol{\alpha})\left(\prod_{k=1}^{N}p_{\Phi_k}(\phi_k)\mathrm{d}\phi_k\right)\mathrm{d}\boldsymbol{\alpha}$$

After simple algebra

$$R(t,t+\tau)=2\sum_{i=1}^{N}\sum_{j=1}^{N}\int_A\sqrt{2H(\omega_i,\boldsymbol{\alpha})S(\omega_i,t)\Delta\omega}\sqrt{2H(\omega_j,\boldsymbol{\alpha})S(\omega_j,t+\tau)\Delta\omega}p_A(\boldsymbol{\alpha})\mathrm{d}\boldsymbol{\alpha}$$
$$\times\int_0^{2\pi}\overset{N-\text{fold}}{\ldots}\int_0^{2\pi}\cos\left(\omega_i t+\phi_i\right)\cos\left(\omega_j(t+\tau)+\phi_j\right)\left(\prod_{k=1}^{N}p_{\Phi_k}(\phi_k)\mathrm{d}\phi_k\right)= \tag{20}$$
$$=\sum_{j=1}^{N}\int_A H(\omega_j,\boldsymbol{\alpha})p_A(\boldsymbol{\alpha})\mathrm{d}\boldsymbol{\alpha}\,2\sqrt{S(\omega_j,t)}\sqrt{S(\omega_j,t+\tau)}\Delta\omega\cos\left(\omega_j\tau\right)$$

Taking into account equation (3), the condition (15) , the limit of equation (20) as $\Delta\omega\to 0$ and $N\to\infty$ will lead to equation (5).

Interestingly, in principle any real positive function satisfying equation (15) can be used for controlling the variability of the simulated process.

4. Butterworth filter

Experimental data of random processes (e.g. earthquake, wind or ocean waves) manifest quite different (joint) frequency distributions, therefore $H(\omega,\boldsymbol{\alpha})$ can be determined considering the distribution of the energy around the expected vale for each frequency. To follow this approach is necessary a large number of data that make this approach practically unfeasible. An alternative strategy is to consider synthetic parameters defining the variability of the energy distribution such as the bandwidths and central frequency. To this aim the following pass-band Butterworth filter will be adopted:

$$H_B(\omega,\alpha_1,\alpha_2)=\frac{1}{2\alpha_1\left[1+\left(\frac{\alpha_2-\omega}{\alpha_1}\right)^{2j}\right]} \tag{21}$$

Where $j=1,2,...,n$ is a positive integer number defining the order of the filter, α_1 and α_2 are the random filter parameters defining respectively the bandwidth and the central frequency. Figure 1a shows for selected $\alpha_1=20\,\text{rad/s}$ and $\alpha_2=40\,\text{rad/s}$ the influence of the order of the filter j while Figure 1b shows the influence of the bandwidth parameter on the shape of the filter.

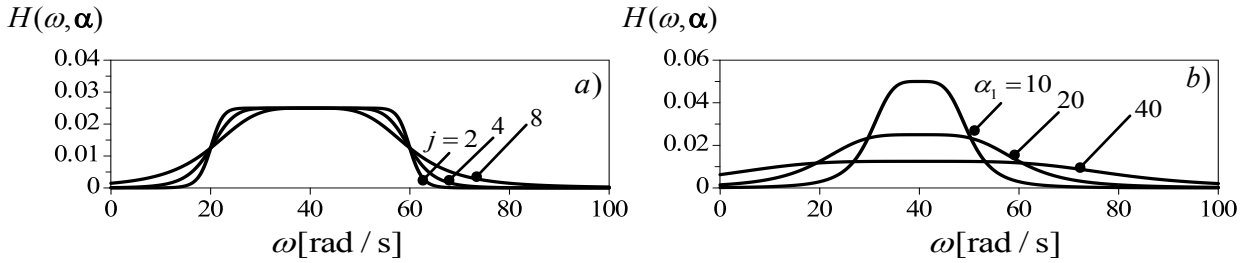

Figure 1. Butterworth filter for (a) different orders and (b) bandwidth ($\alpha_2=40\,\text{rad/s};\ j=2$)

The distribution of the filter parameters α_1 and α_2 can be defined through experimental data measuring the central frequency and bandwidth of the squared Fourier spectrum of the recorded samples. In the case in which the experimental data are not enough to define a proper distribution of the data α_1 and α_2 will be assumed as statistical independent and uniformly distributed. Therefore,

$$p_A(\boldsymbol{\alpha})=p_{A_1}(\alpha_1)p_{A_2}(\alpha_2)=\frac{1}{\alpha_{u1}-\alpha_{l1}}\frac{1}{\alpha_{u2}-\alpha_{l2}}, \tag{22}$$

where α_{ui} and α_{li} ($i=1,2$) represents the upper and lower bounds of the random variables α_1 and α_2. The simulation formula will be then modified as follows

$$f_H(t)=\sqrt{2}\sum_{j=1}^{N}\sqrt{2C(\omega)H_B(\omega_j,\alpha_1,\alpha_2)S(\omega_j,t)\Delta\omega}\cos\left(\omega_j t+\phi_j\right), \tag{23}$$

where the function $C(\omega)$ is introduced to satisfy equation (15) , i.e.

$$C(\omega)=\left(\frac{1}{\alpha_{u1}-\alpha_{l1}}\frac{1}{\alpha_{u2}-\alpha_{l2}}\int_{\alpha_{l1}}^{\alpha_{u1}}\int_{\alpha_{l2}}^{\alpha_{u2}}H_B(\omega,\alpha_1,\alpha_2)\mathrm{d}\alpha_1\mathrm{d}\alpha_2\right)^{-1} \tag{24}$$

It is noted that being $C(\omega)$ function of the circular frequency ω the pass-band filter will be distorted, however being $C(\omega)$ a smooth function the main features of the filters will be preserved.

5. Numerical results

In this section stationary and non-stationary samples are generated following the traditional spectral representation method and the proposed one enhancing the variability. Consider the stationary case first. It is assumed that the process is zero-mean, Gaussian with power spectral density function defined by the Clough-Penzien model, that is

$$S(\omega) = S_0 \frac{\left(1+4\zeta_g^2\left(\frac{\omega}{\omega_g}\right)^2\right)}{\left(1-\left(\frac{\omega}{\omega_g}\right)^2\right)^2+4\zeta_g^2\left(\frac{\omega}{\omega_g}\right)^2} \frac{\left(\frac{\omega}{\omega_f}\right)^4}{\left(1-\left(\frac{\omega}{\omega_f}\right)^2\right)^2+4\zeta_f^2\left(\frac{\omega}{\omega_f}\right)^2} \tag{25}$$

with parameters

$$\omega_g = 20 \text{ rad/s}; \quad \zeta_g = 0.6; \quad \omega_f = 0.1\omega_g; \quad \zeta_f = \zeta_g \tag{26}$$

and

$$S_0 = \frac{\sigma^2}{2\pi\omega_g\left(2\zeta_g+\frac{1}{2\zeta_g}\right)}; \qquad \sigma = 100 \text{ cm/s}^2. \tag{27}$$

Samples of the stationary processes have been simulated using equation (11) by substituting $S(\omega,t)$ with $S(\omega)$ and depicted in Figure 2a. The power spectral density are then randomized using the Butterworth pass-band filter defined in equation (21), in which the random variables α_1 and α_2 are assumed statistical independent and uniformly distributed. Pertinent selected parameters of the distributions are

$$\alpha_{l1} = 10 \text{ rad/s}; \quad \alpha_{u1} = 80 \text{ rad/s}; \quad \alpha_{l2} = 18 \text{ rad/s}; \quad \alpha_{u1} = 40 \text{ rad/s}. \tag{28}$$

Samples of the random processes with enhanced variability are then simulated using equation (23). It is noted that each individual sample requires *N+2* realizations of independent uniformly distributed random variables (*N* phase angles ϕ_j and 2 filter parameter α_1 and α_2). Figure 2b shows three simulated trajectories. The effect of the Butterworth filter in the simulation of the process is more appreciated in Figures 3 where the squared modulus of the Fourier transform of the simulated samples is depicted. It is noted that the samples simulated from the traditional spectral-representation method exhibit Fourier spectra very similar to each other, while the proposed modification lead to spectra possessing clearly visible different distributions.

Comparison with the target power spectral density is shown in Figure 4. It is noted that the ensemble average power spectra determined using 500 samples oscillates around the target spectrum.

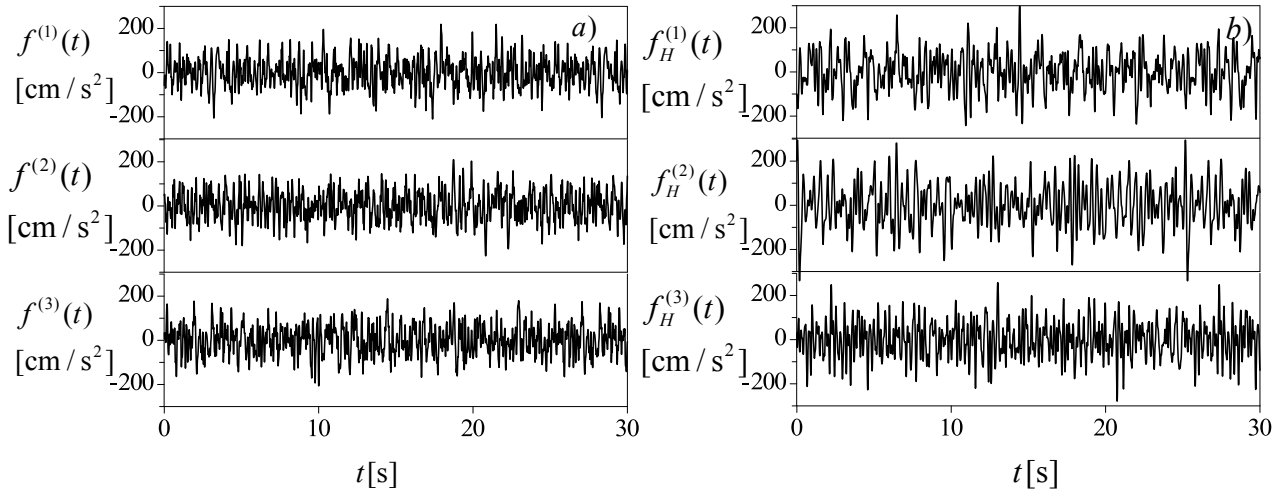

Figure 2. Simulated trajectories of the zero-mean Gaussian, stationary process through a) spectral representation method b) proposed with enhanced variability.

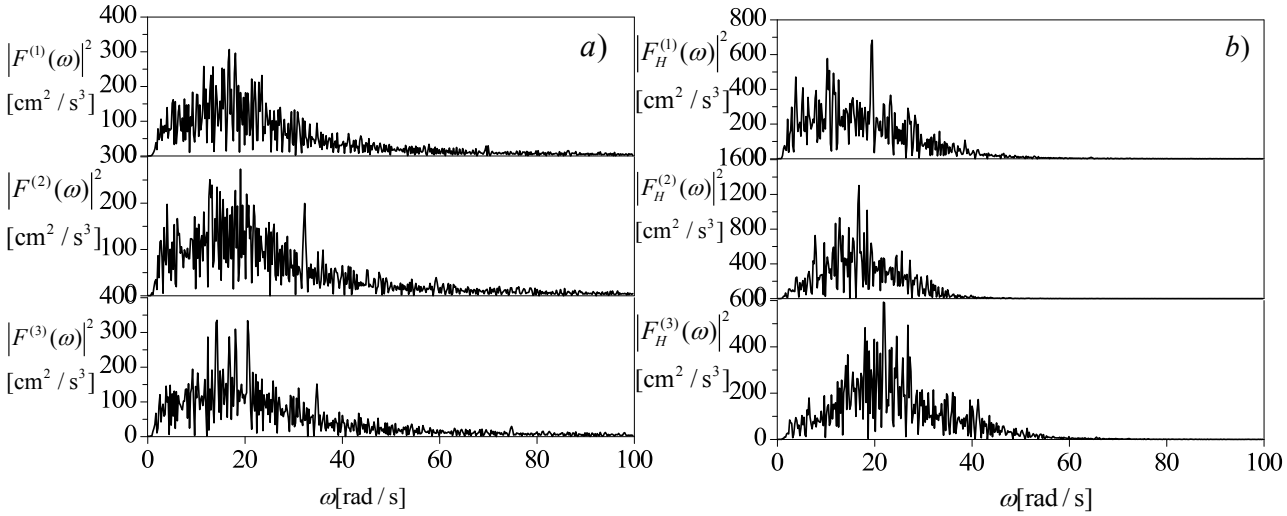

Figure 3. Squared Fourier transform of the simulated samples a) spectral representation method b) proposed with enhanced variability.

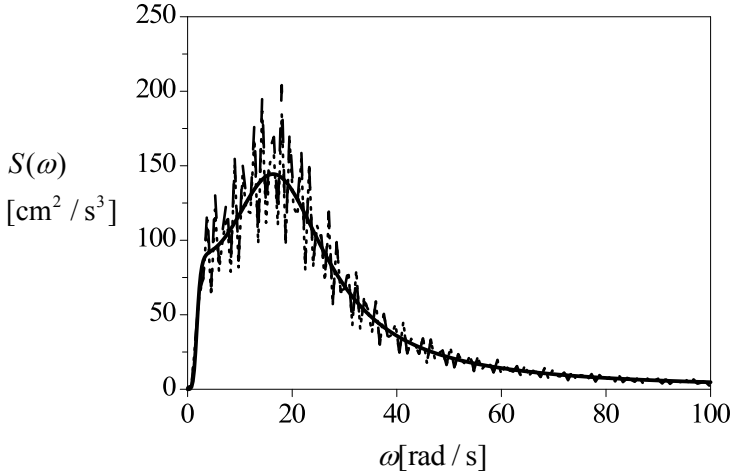

Figure 4. Comparison between the target power spectral density function (solid line), the ensemble averaged determined by using the spectral representation method (dotted line) and the SRM with enhanced variability (dash-dotted line).

The non stationary case is then investigated. The evolutionary power spectral density defined in equation (29) is selected for this purpose

$$S(\omega,t)=A(t)^2 S_0(t)\frac{\left(1+4\zeta_g^2(t)\left(\frac{\omega}{\omega_g(t)}\right)^2\right)}{\left(1-\left(\frac{\omega}{\omega_g(t)}\right)^2\right)^2+4\zeta_g^2(t)\left(\frac{\omega}{\omega_g(t)}\right)^2}\frac{\left(\frac{\omega}{\omega_f(t)}\right)^4}{\left(1-\left(\frac{\omega}{\omega_f(t)}\right)^2\right)^2+4\zeta_f^2(t)\left(\frac{\omega}{\omega_f(t)}\right)^2} \tag{29}$$

pertinent parameters used in this numerical example include:

$$\omega_g(t)=20-7\frac{t}{30};\quad \zeta_g(t)=0.6-0.2\frac{t}{30};\quad \omega_f(t)=0.1\omega_g(t);\quad \zeta_f(t)=\zeta_g(t); \tag{30}$$

and

$$A(t)=a_1 t\exp\left(-a_2 t\right);\quad a_1=0.68\,\mathrm{s}^{-1};\quad a_2=1/4\,\mathrm{s}^{-1}. \tag{31}$$

Furthermore

$$S_0(t)=\frac{\sigma^2}{2\pi\omega_g(t)\left(2\zeta_g(t)+\frac{1}{2\zeta_g(t)}\right)};\quad \sigma=100\,\mathrm{cm}/\mathrm{s}^2. \tag{32}$$

Samples of the non-stationary processes simulated using equations (11) and (23) are depicted in Figures 5 and their related squared Fourier transform in Figure 6. Also in this case it can be appreciated as the random filter modifies the distribution of each sample.

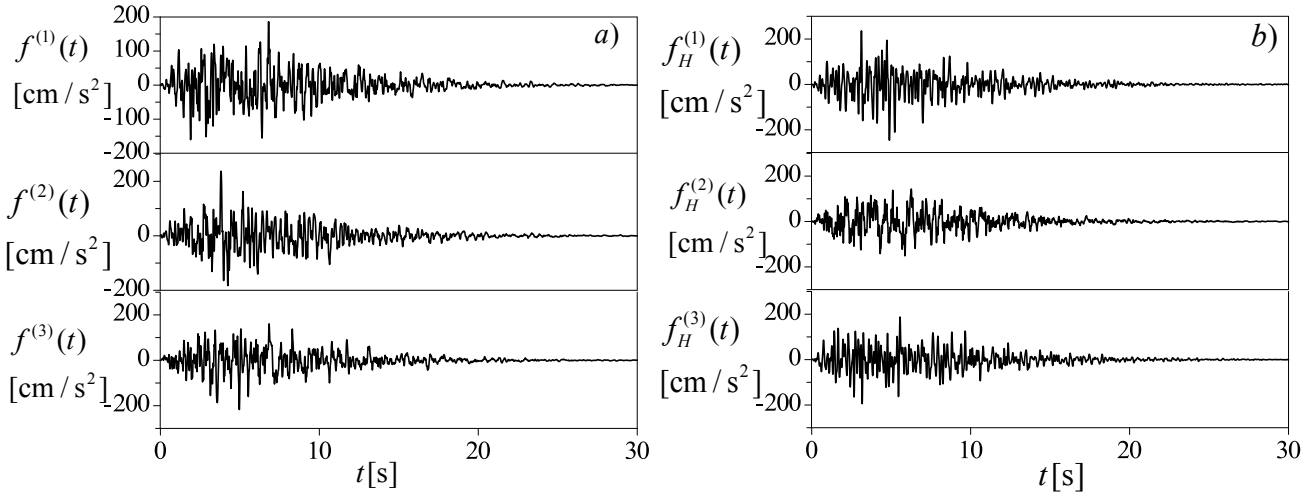

Figure 5. Simulated trajectories of the zero-mean Gaussian, non-stationary process through a) spectral representation method b) proposed with enhanced variability.

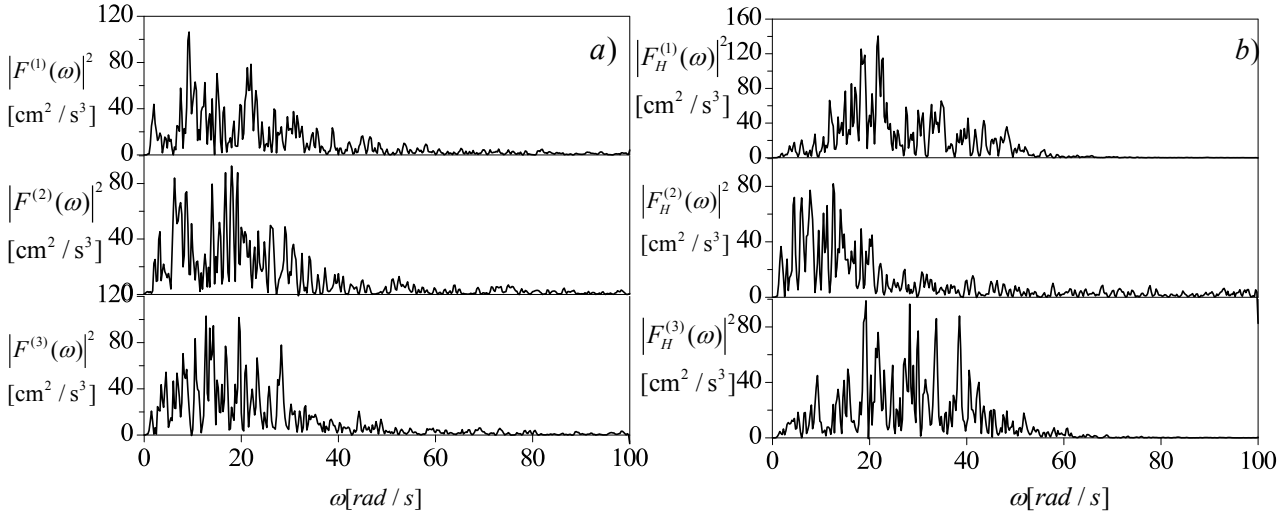

Figure 6. Squared Fourier transform of the simulated samples a) spectral representation method b) proposed with enhanced variability.

Comparisons with the target spectrum is shown in Figures 7 where the marginal distributions (Cohen, 1989)

$$\lambda(t) = \int_0^{\omega_N} 2S(\omega,t)\mathrm{d}\omega\,; \qquad S(\omega) = \frac{1}{t_f}\int_0^{t_f} 2S(\omega,t)\mathrm{d}t \tag{33}$$

are compared respectively with the ensemble average of the squared samples $E[f(t)^2]$, $E[f_H(t)^2]$ and with ensemble average of the squared Fourier transform $E[|F(\omega)|^2]$, $E[|F_H(\omega)|^2]$. The comparison shows the excellent agreement between the simulated and the target ones

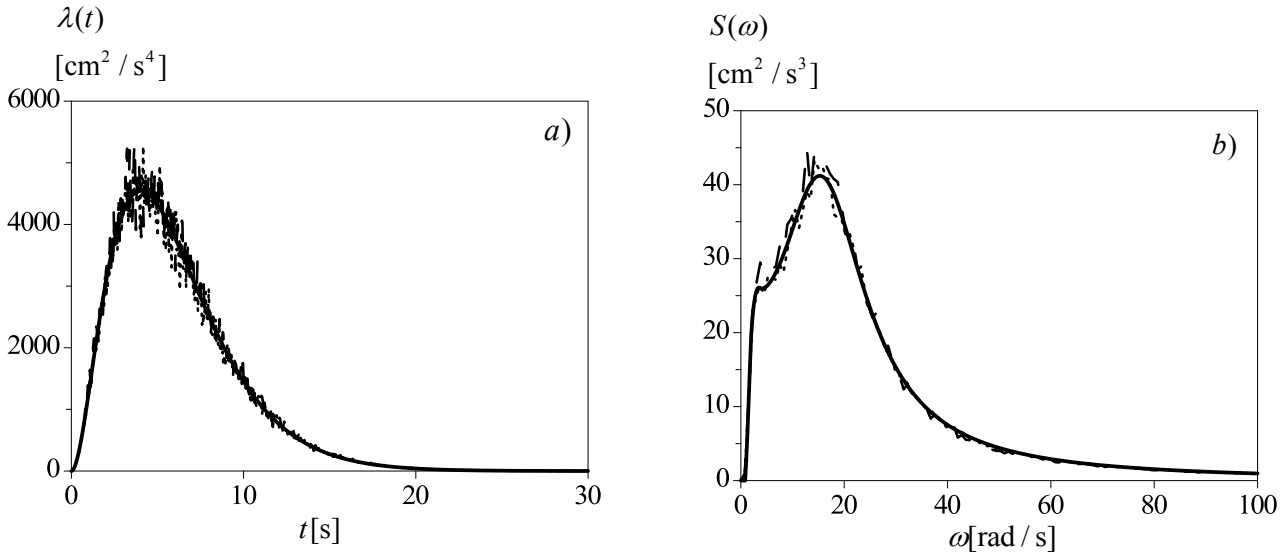

Figure 7. Comparison between the marginal distribution of the evolutionary power spectral density function a) mean instantaneous energy and b) energy density spectrum; target (solid line), the ensemble averaged determined by using the spectral representation method (dotted line) and SRM with enhanced variability (dash-dotted line).

The influence of the enhanced spectrum variability is then investigated through the Monte Carlo study of the distribution of peaks value. Figure 8 shows the comparison between the mean value of the peak of the stationary (Figure 8a) and non-stationary process (Figure 8b). Interestingly both the simulation tends to very similar value and the rate of convergence is comparable. Figures 9 shows the variance of the distribution of maxima. It is noted that the SRM with enhanced variability leads to larger values of the variance. Finally the distributions of maxima along its cumulative distribution are depicted in Figures 10 and 11. It is noted that in both stationary and non stationary case the SRM with enhanced variability leads to wider distribution and as a consequence sensitive different values of the tails of the distribution.

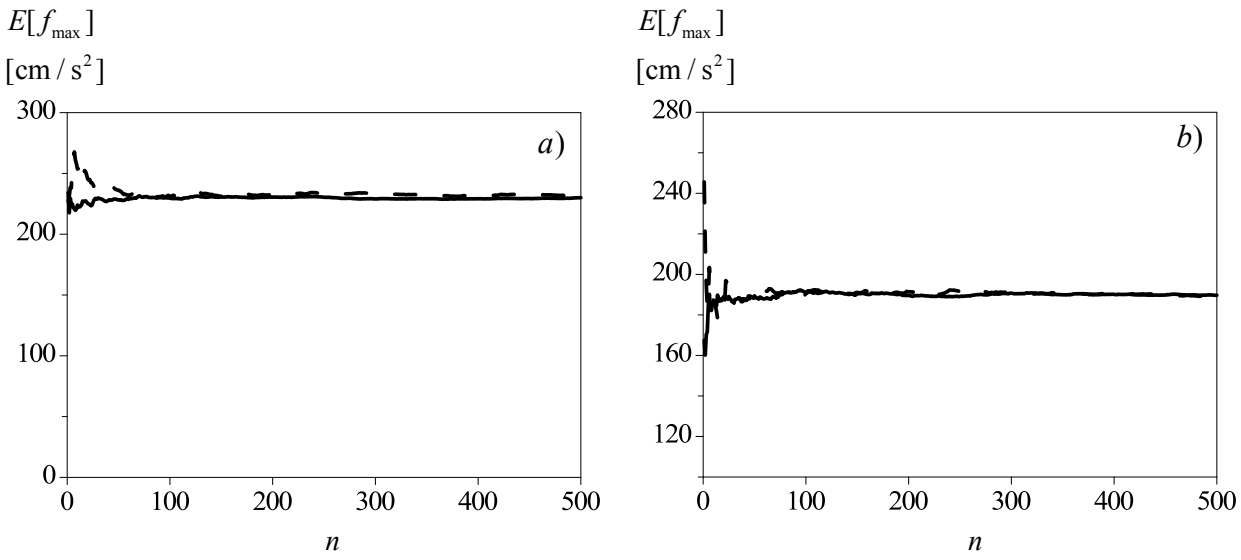

Figure 8. Convergence of the mean value of the peak versus the number of samples *n* for the a) stationary and b) non-stationary process: traditional SRM (solid line), SRM with enhanced variability (dash-dotted line).

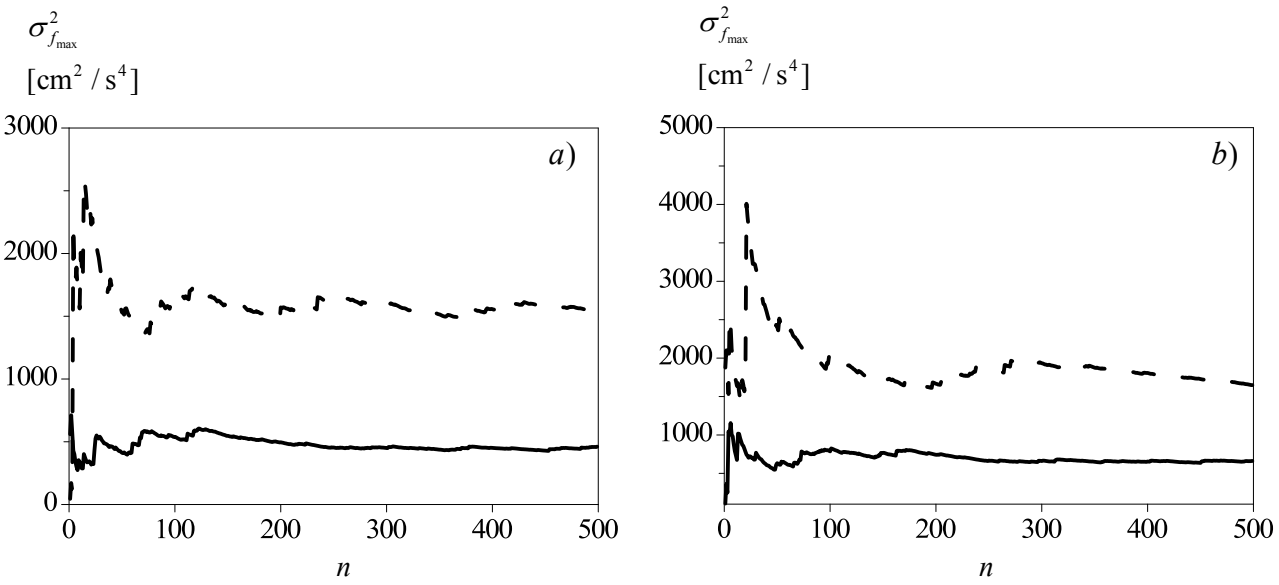

Figure 9. Convergence of the variance of the peak value versus the number of samples *n* for the a) stationary and b) non-stationary process: traditional SRM (solid line), SRM with enhanced variability (dash-dotted line).

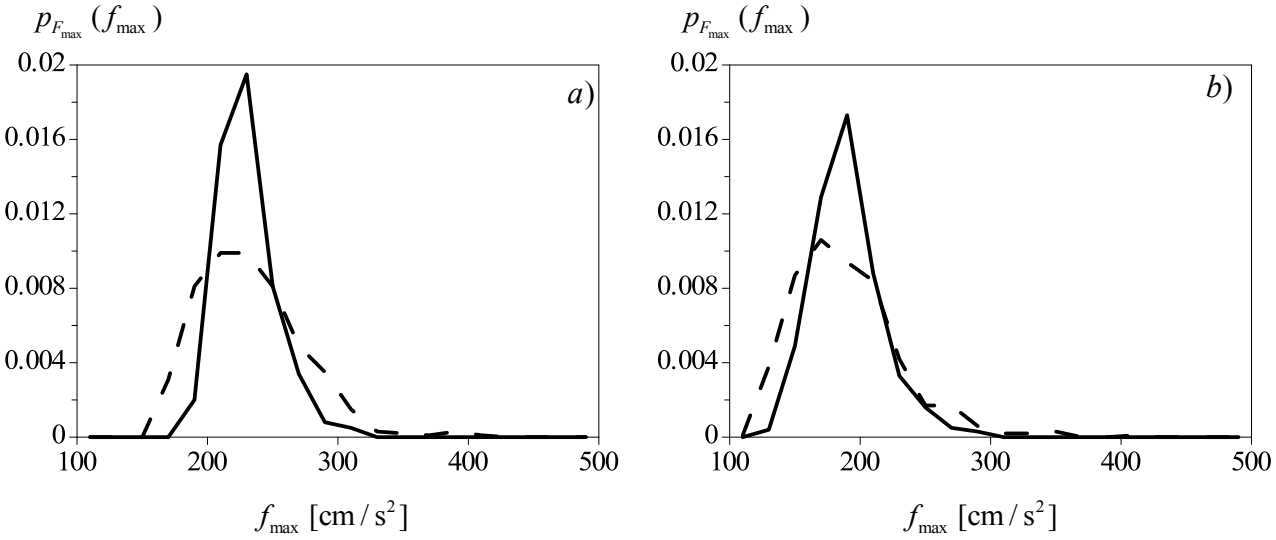

Figure 10. Comparison between the distribution of peaks for the a) stationary and b) non-stationary process: traditional SRM (solid line), SRM with enhanced variability (dash-dotted line).

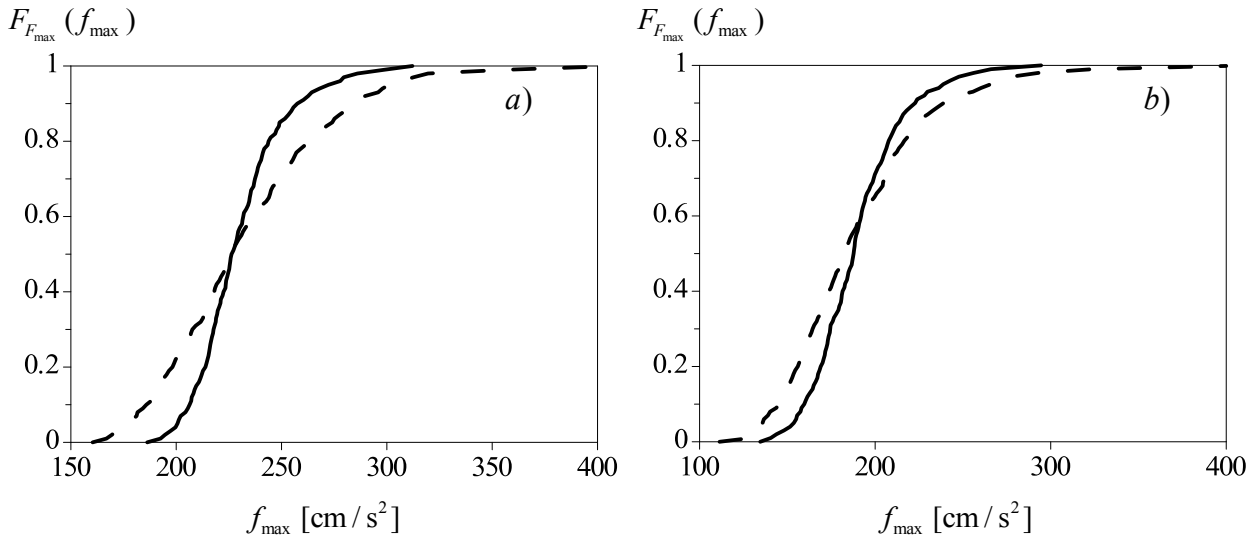

Figure 11. Comparison between the cumulative distribution of peaks for the a) stationary and b) non-stationary process: traditional SRM (solid line), SRM with enhanced variability (dash-dotted line).

6. Concluding remarks

In this paper the traditional spectral-representation-method for simulating stochastic processes is revisited. A modification aimed to control the variability of the simulated samples of the random process is proposed. Specifically a Butterworth pass-band filter with random parameters has been included in the simulation formula to generate samples with different Fourier spectra. It has been shown that the use of this filter do not alter the convergence of the traditional spectral representation method, offering a possible simulation strategy whereas it is required a variability larger than those currently offered by the traditional simulation technique. Comparison between the traditional spectral representation method and the enhanced variability introduced in this paper showed how the randomized power spectral density influence the ensemble simulated samples. Remarkably the peak distribution is significantly sensible to the spectrum variability and should be carefully considered when reliability analyses are performed. It is also expected in general that the spectrum variability influence the features of the process non-linearly related to the power spectrum.

7. References

Cacciola P and Zentner I, Generation of response-spectrum-compatible artificial earthquake accelerograms with random joint time–frequency distributions Probabilistic Engineering Mechanics (28), 52-58, 2012

Cohen L. Time-Frequency Distributions – A Review. Proceedings of the IEEE; 77(7): 941-981,1989.

Deodatis, G. Non-stationary stochastic vector processes: seismic ground motion applications. Probabilistic Engineering Mechanics 11: 149-168, 1996.

Li J, Yan Q ,Chen JB, Stochastic modeling of engineering dynamic excitation for stochastic dynamics of structures, Probabilistic Engineering Mechanics, 27, 19-28, 2012.

Pousse, G., Bonilla, L.F., Cotton, F., Margerin, L., Nonstationary Stochastic Simulation of String Ground Motion Time Histories Including Natural Variability: Application to the K-Net Japanes Database, Bullettin of the Seismological Society of America, 96(6), 2103-2117, 2006.

Priestley, M.B. Evolutionary spectra and non-stationary processes, Journal of the Royal Statistical Society, Series B, Methodological, 27(2), 204-237, 1965.

Rezaeian S and Der Kiureghian A, Simulation of synthetic ground motions for specified earthquake and site characteristics, Earthquake Engineering and Structural Dynamics, 39, 1155-1180, 2010

Schillinger D and Papadopoulos V, The method of separation: a novel approach for accurate estimation of evolutionary power spectra, Computational methods in Stochastic Dynamics, Papadrakakis M, Stefanou G, Papadopolous V eds. Springer, 209-228, 2011.

Shinozuka, M. and Deodatis, G. "Stochastic Process Models for Earthquake Ground Motion," Probabilistic Engineering Mechanics, 3, (3), 114-123, 1988

Spanos PD, Failla G, Evolutionary spectra estimation using wavelets, Journal of Engineering Mechanics (ASCE), 130(8), 952-960,2004.

Viallet E., Humbert N. Considerations on the use of natural and artificial time histories for seismic transient non-linear analyses of structures and variability assessment. Proceedings of SMiRT 19, Toronto, Canada, 2007.